Boosting CO_2 Methanation over Ni-based Catalysts via La-Al Mixed Oxide Synergy

SUPPORTING INFORMATION

R. B. Machado-Silva[a], L.M. Andrés-Olmos[a], N. Kosinov[b], E. Hensen[b], A. Chica[a]

[a] Instituto de Tecnología Química (Universitat Politècnica de València-Consejo Superior de Investigaciones Científicas), Avd. de los Naranjos s/n, 46022 Valencia (Spain).
[b] Laboratory of Inorganic Materials and Catalysis, Department of Chemical Engineering and Chemistry, Eindhoven University of Technology, Helix, STW 3.33, Het Kranenveld 14, 5612 AZ Eindhoven, (The Netherlands).

*Corresponding author: Antonio Chica
Tel.: +34 963 87 70 00 - 78508;
Fax: +34 963 87 78 09.
E-mail address: achica@itq.upv.es

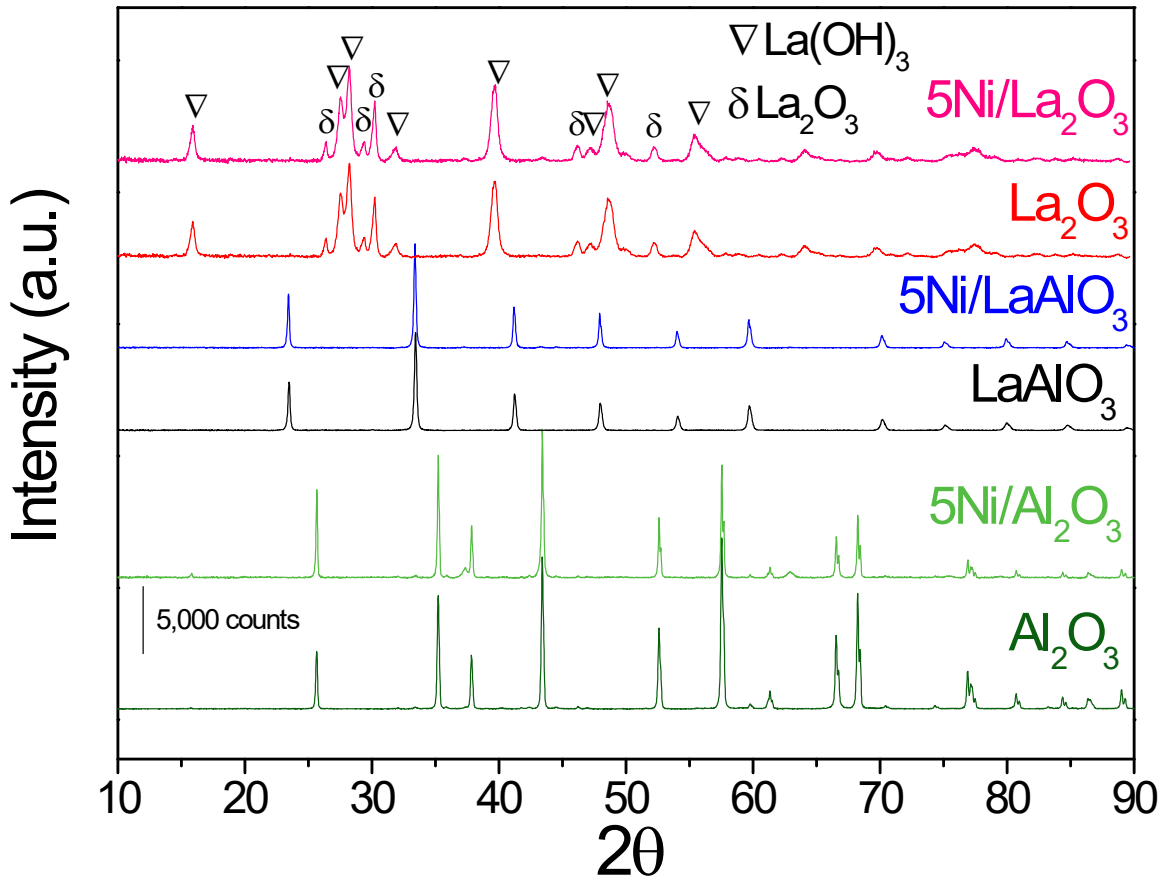

Figure S1. XRD diffractograms of the different supports and equivalent 5% wt. Ni-based catalysts.

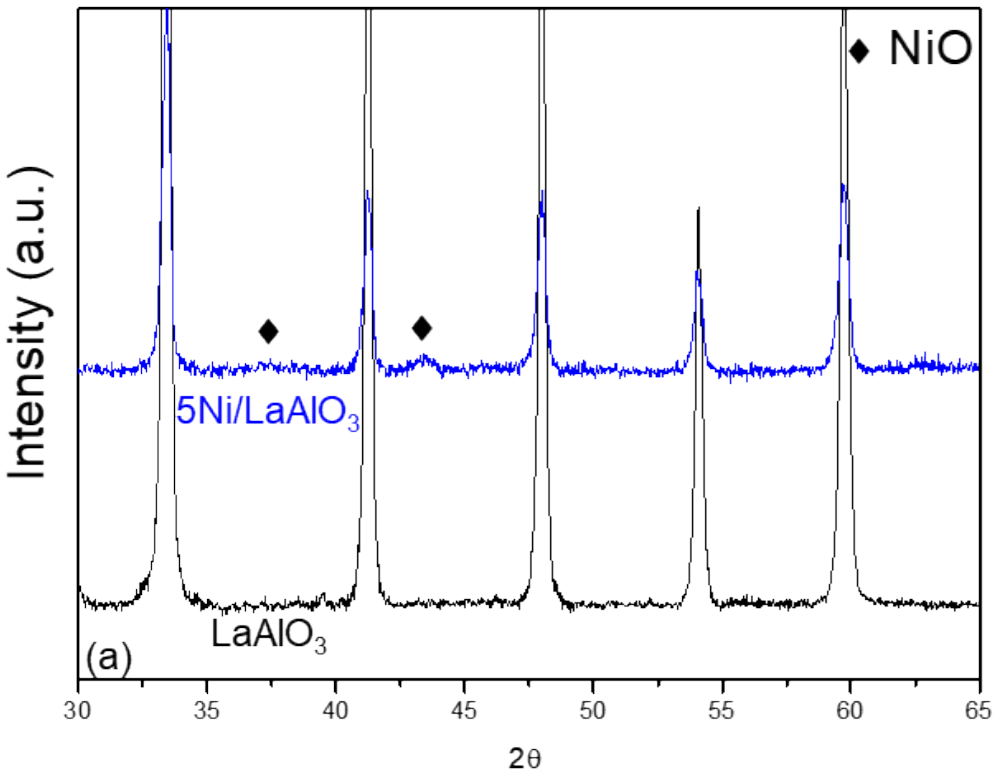
◆ NiO
Intensity (a.u.)
5Ni/LaAlO3
LaAlO3
(a)
30
35
40
45
50
55
60
65
2θ

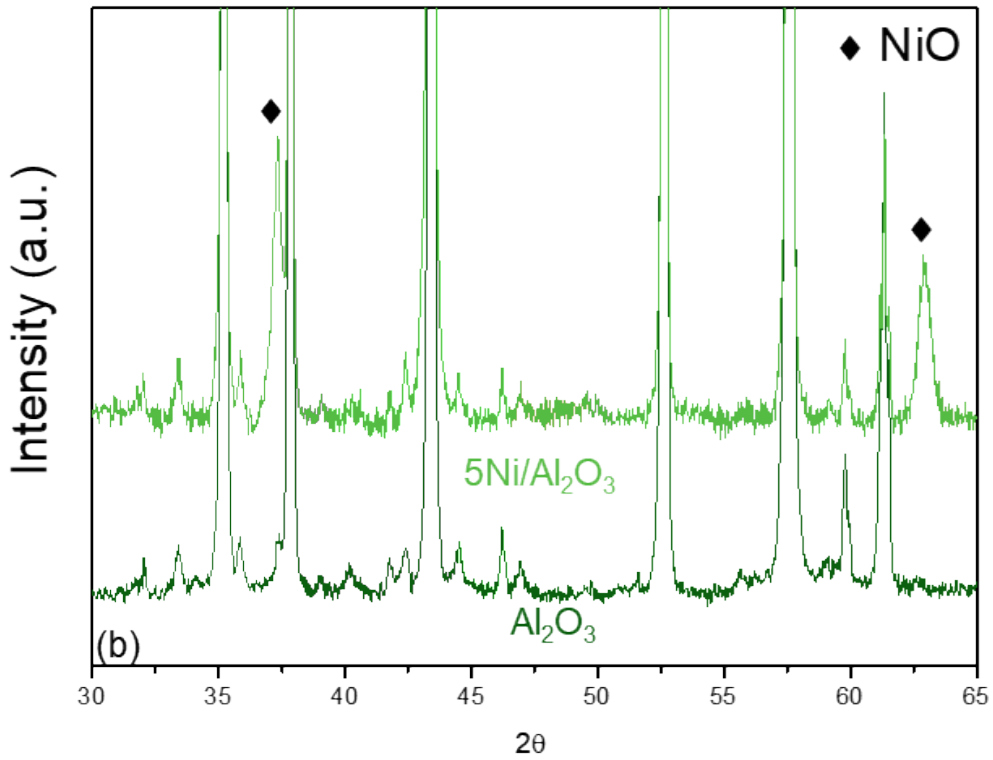
◆ NiO
Intensity (a.u.)
5Ni/Al2O3
Al2O3
(b)
30
35
40
45
50
55
60
65
2θ

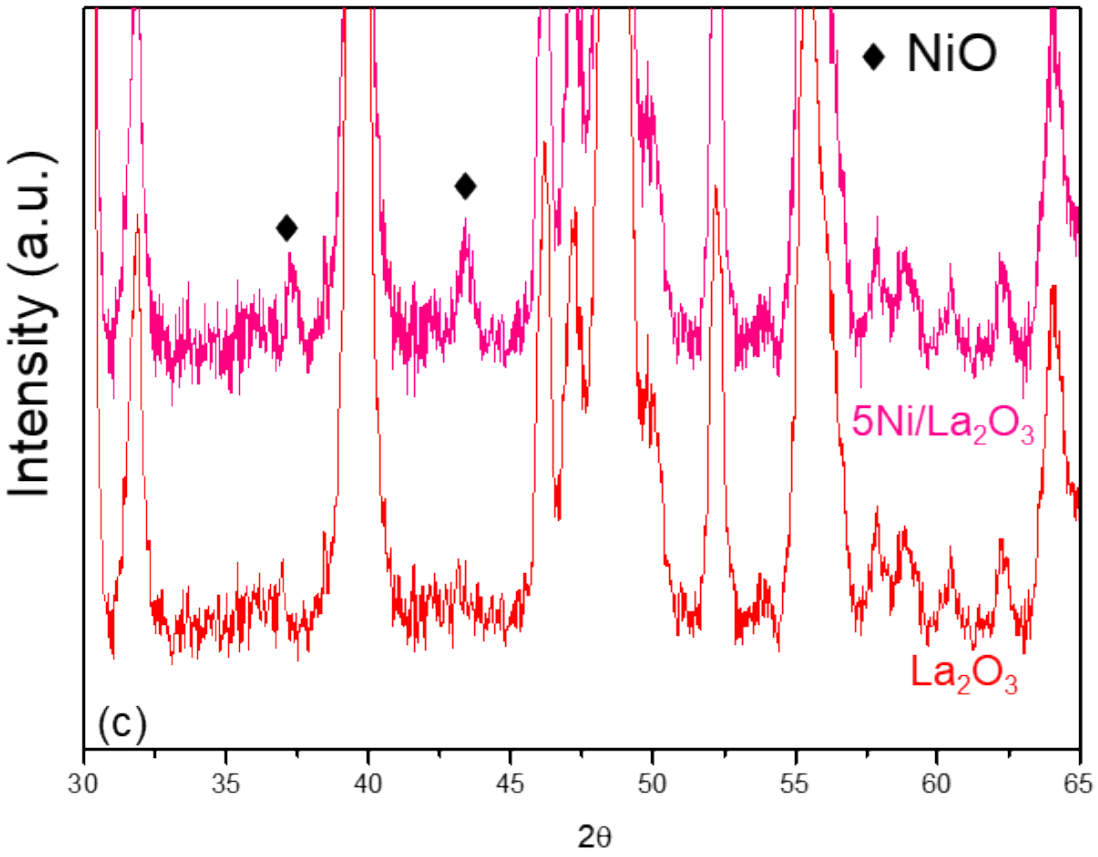

Figure S2. Magnification of specific ranges to highlight the presence of the peaks (♦) associated with the presence of NiO at 2θ = 37.40° and 43.46°.

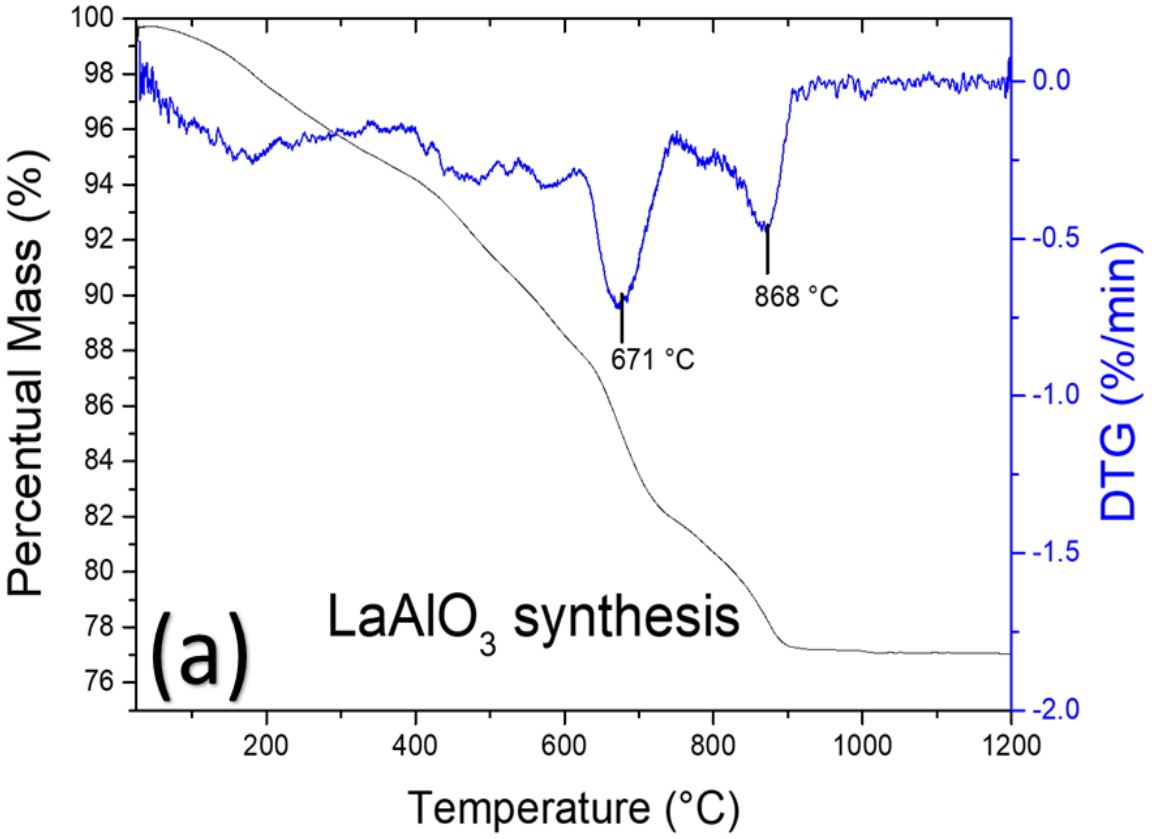
Percentual Mass (%)
DTG (%/min)
Temperature (°C)
671 °C
868 °C
(a)
LaAlO3 synthesis

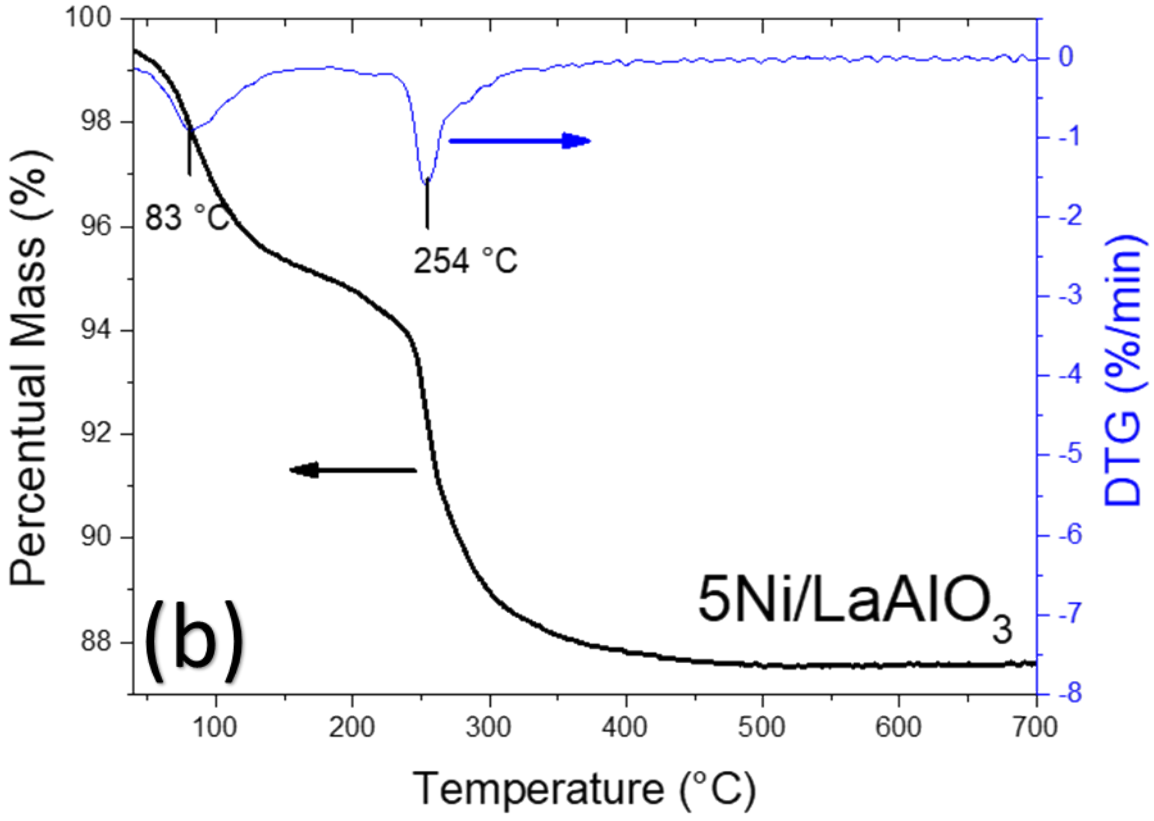
Percentual Mass (%)
DTG (%/min)
Temperature (°C)
83 °C
254 °C
(b)
5Ni/LaAlO3

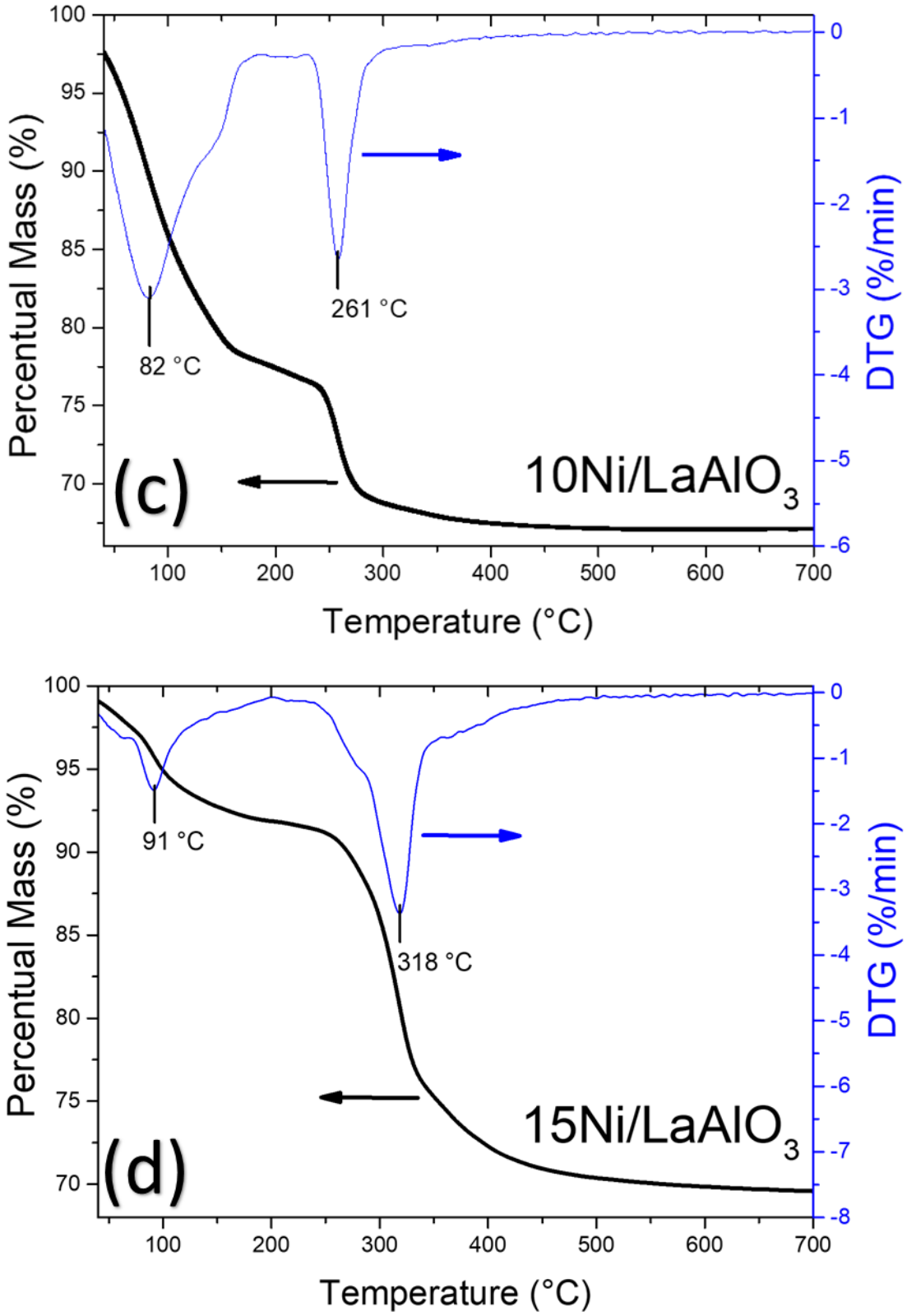

Figure S3. Thermogravimetric differential analysis for: (a) the support precursors for $LaAlO_3$ before the calcination, and the Ni-impregnated $LaAlO_3$ supports with different metallic loadings: (b) 5 wt. %; (c) 10 wt. %; (b) 15 wt. %.

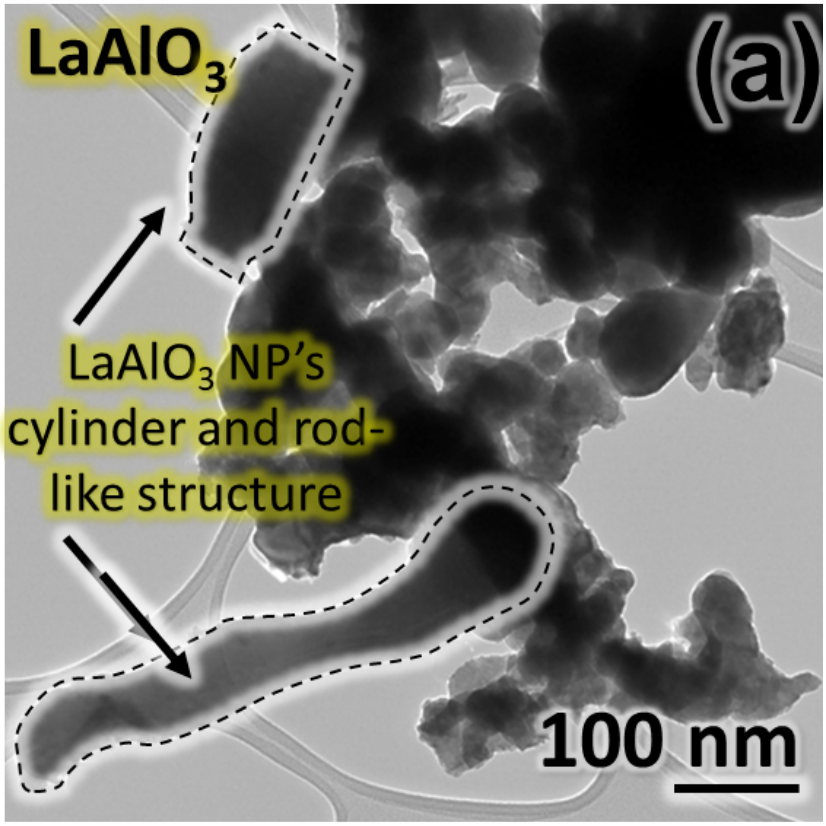
LaAlO3
(a)
LaAlO3 NP's
cylinder and rod-
like structure
100 nm

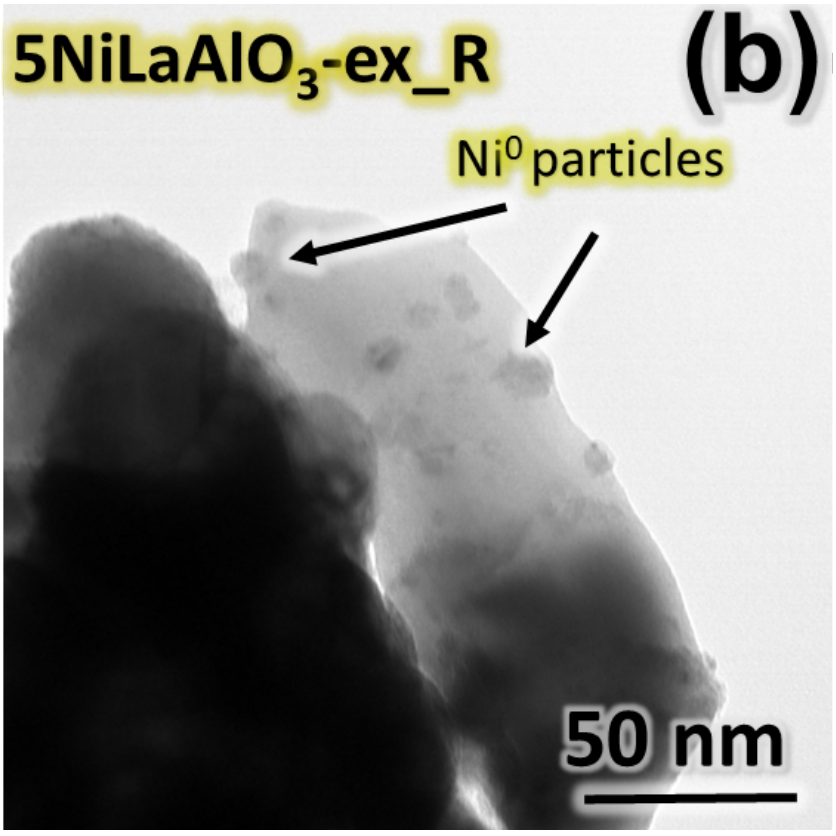
5NiLaAlO3-ex_R
(b)
Ni0 particles
50 nm

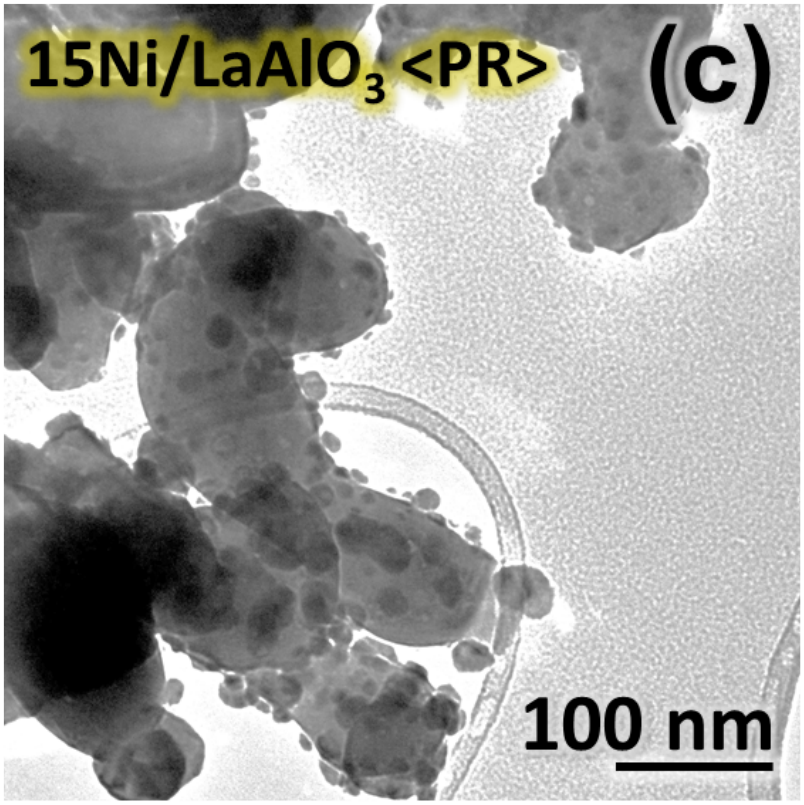

Figure S4. TEM images of: (a) $LaAlO_3$; (b) 5Ni/$LaAlO_3$-ex_R; (c) 15Ni/$LaAlO_3$<PR>.

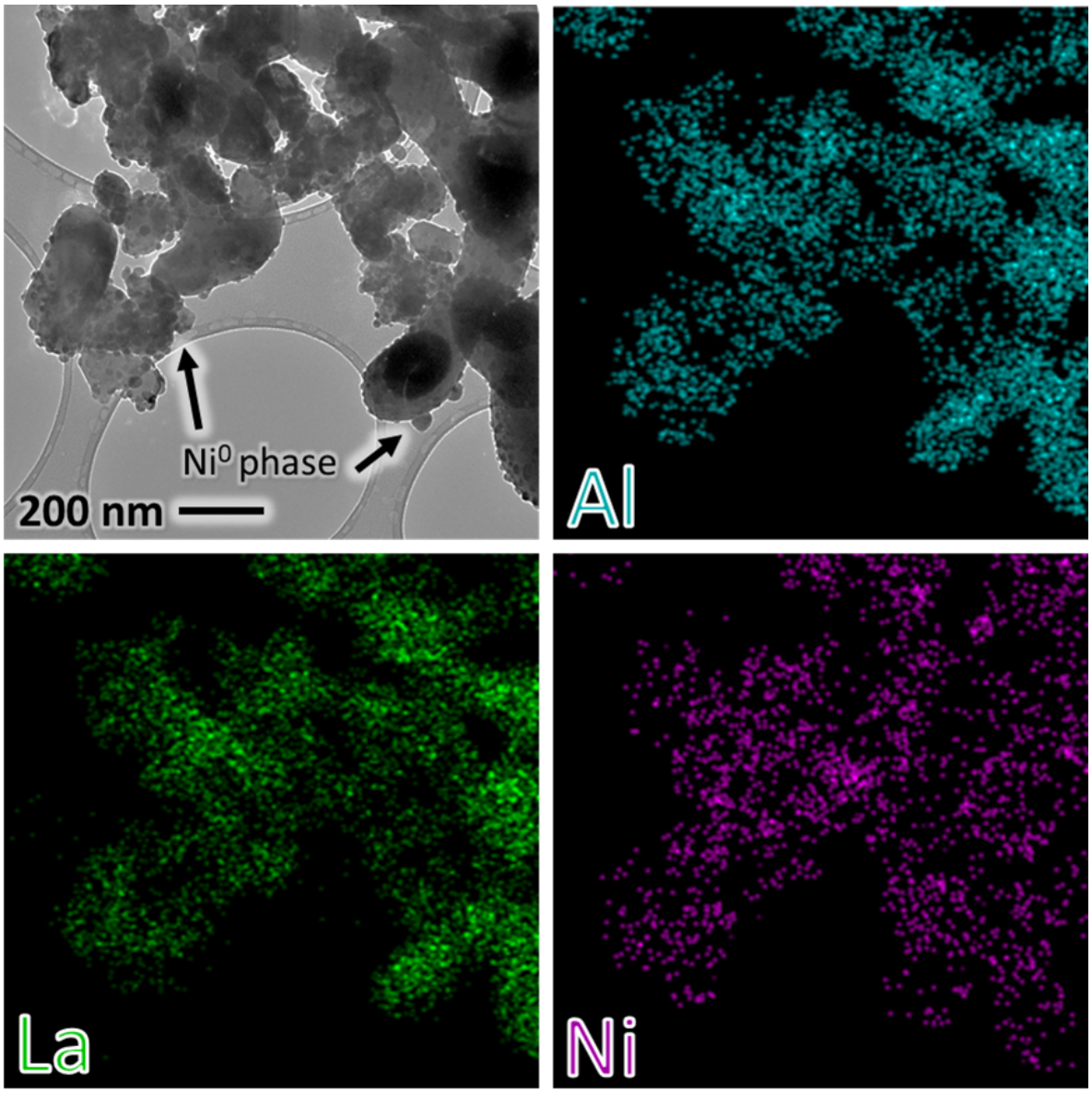

Figure S5. EDS-TEM results for the 15Ni/$LaAlO_3$_R and the response obtained for different elements: Al (cerulean); La (green) and Ni (purple).

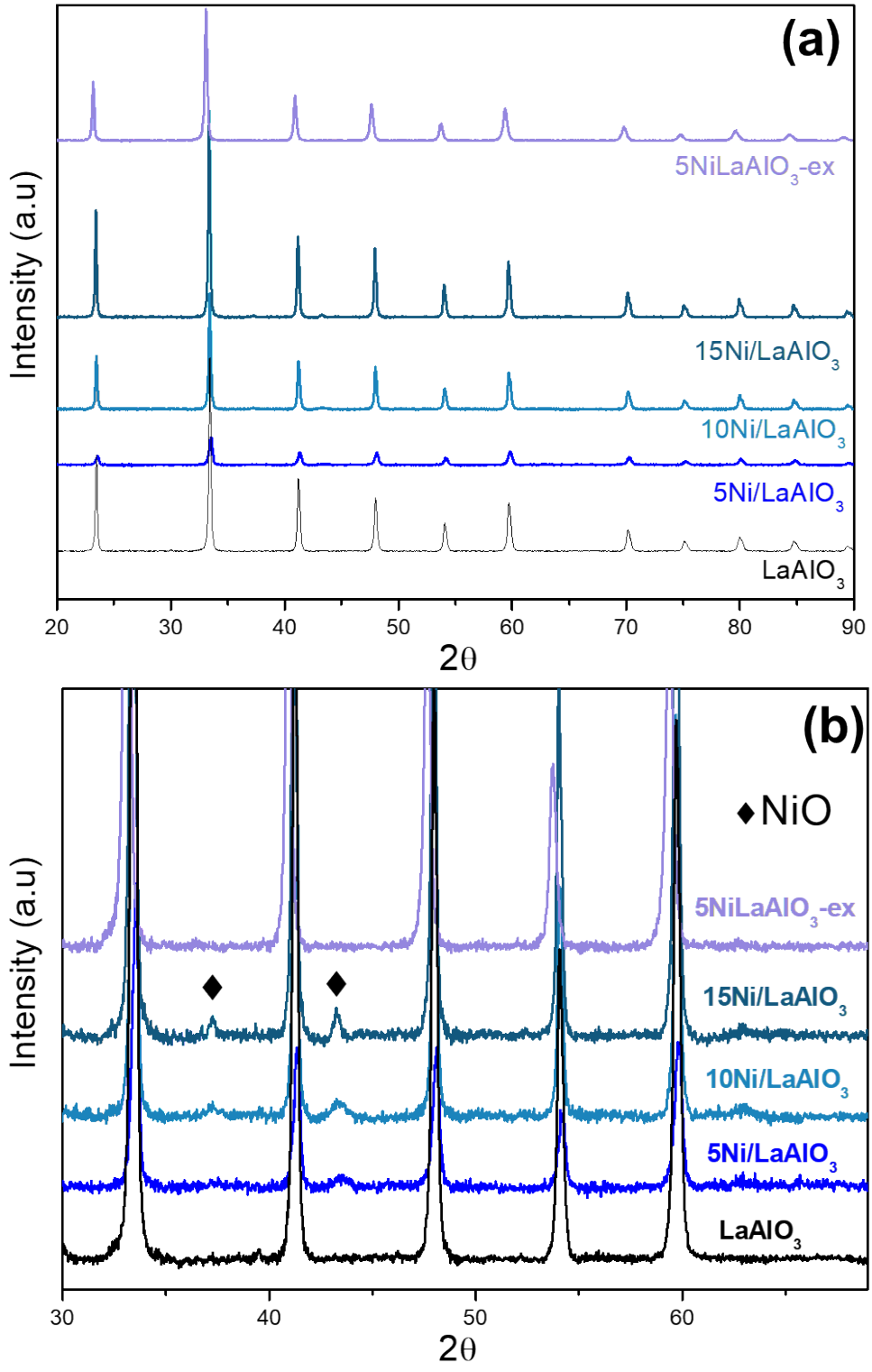

Figure S6. (a) XRD diffractograms of the calcined $LaAlO_3$-based catalysts prepared by different methods and metallic content. (b) Magnification of the region between 2θ = 30° and 70° to highlight diffraction peaks related to the presence of the NiO phase.

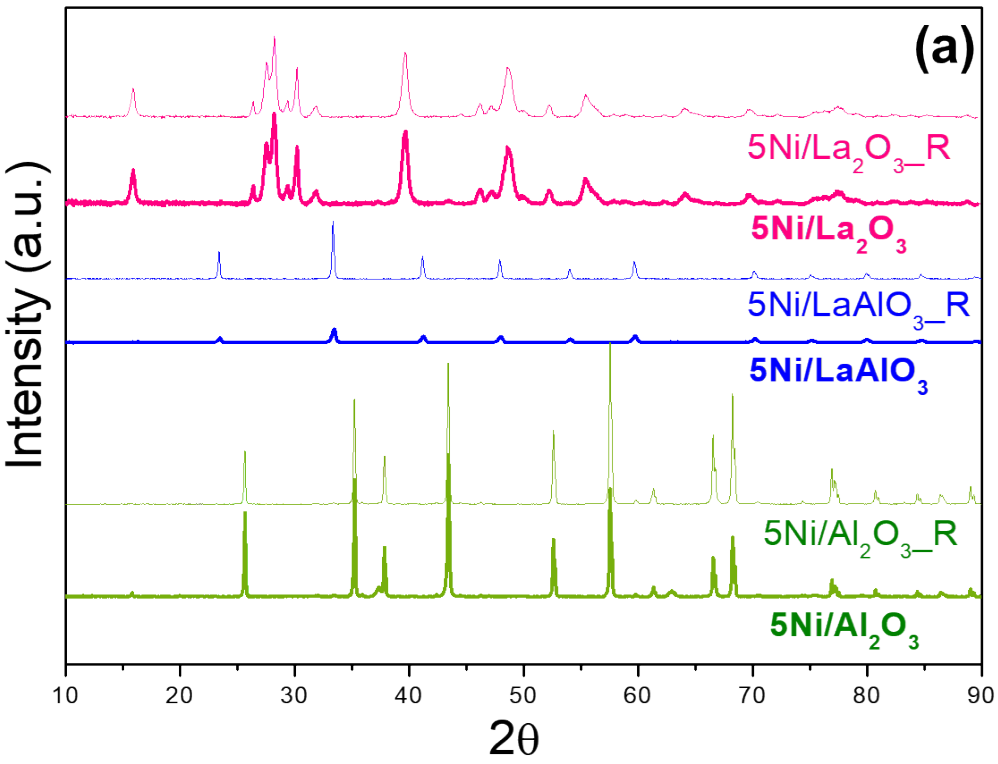
(a)
Intensity (a.u.)
5Ni/La2O3_R
5Ni/La2O3
5Ni/LaAlO3_R
5Ni/LaAlO3
5Ni/Al2O3_R
5Ni/Al2O3
10
20
30
40
50
60
70
80
90
2θ

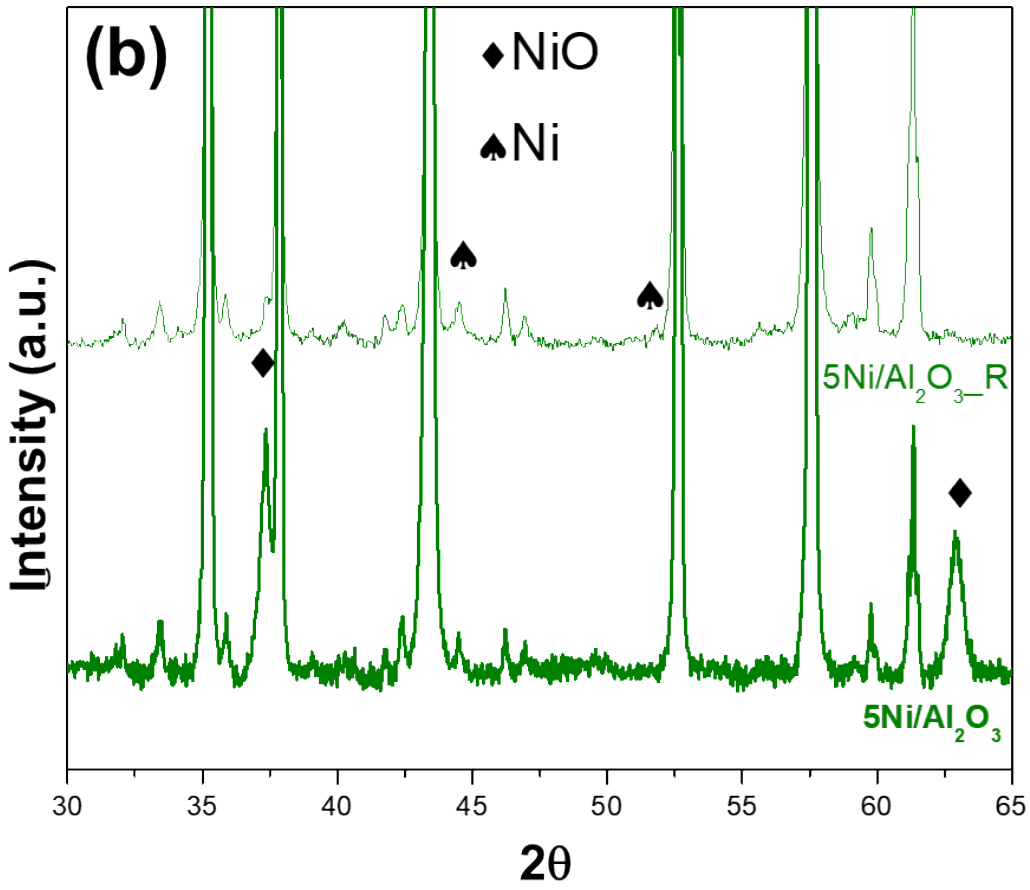
(b)
♦NiO
♠Ni
Intensity (a.u.)
5Ni/Al2O3_R
5Ni/Al2O3
30
35
40
45
50
55
60
65
2θ

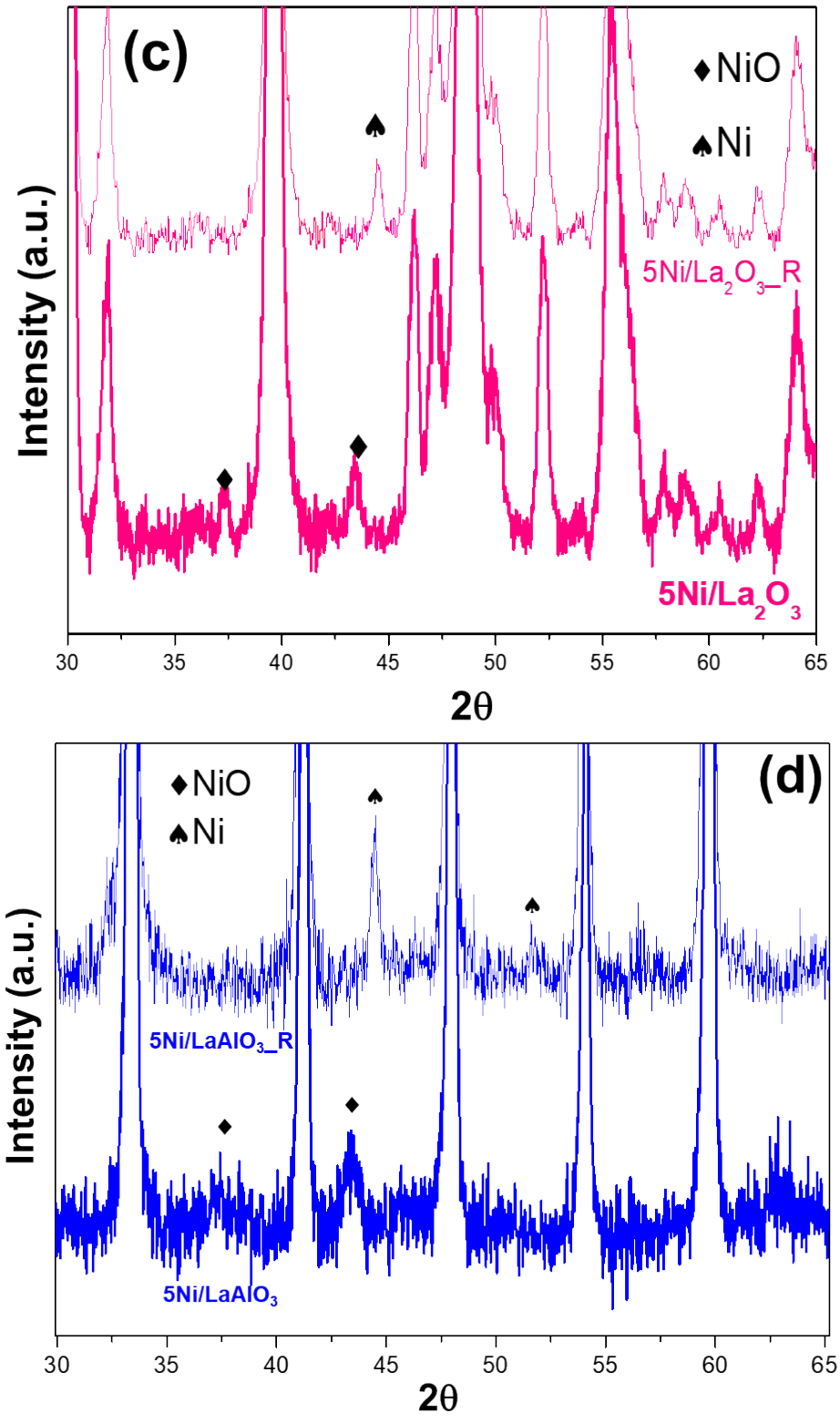

Figure S7. (a) Comparison of the XRD diffractograms of the reduced version of the 5% wt. catalysts with the calcined ones for the different supports and zoom-in of the region between 2θ = 30° and 65° for the (b) 5Ni/Al_2O_3_R and (c) 5Ni/La_2O_3_R catalysts.

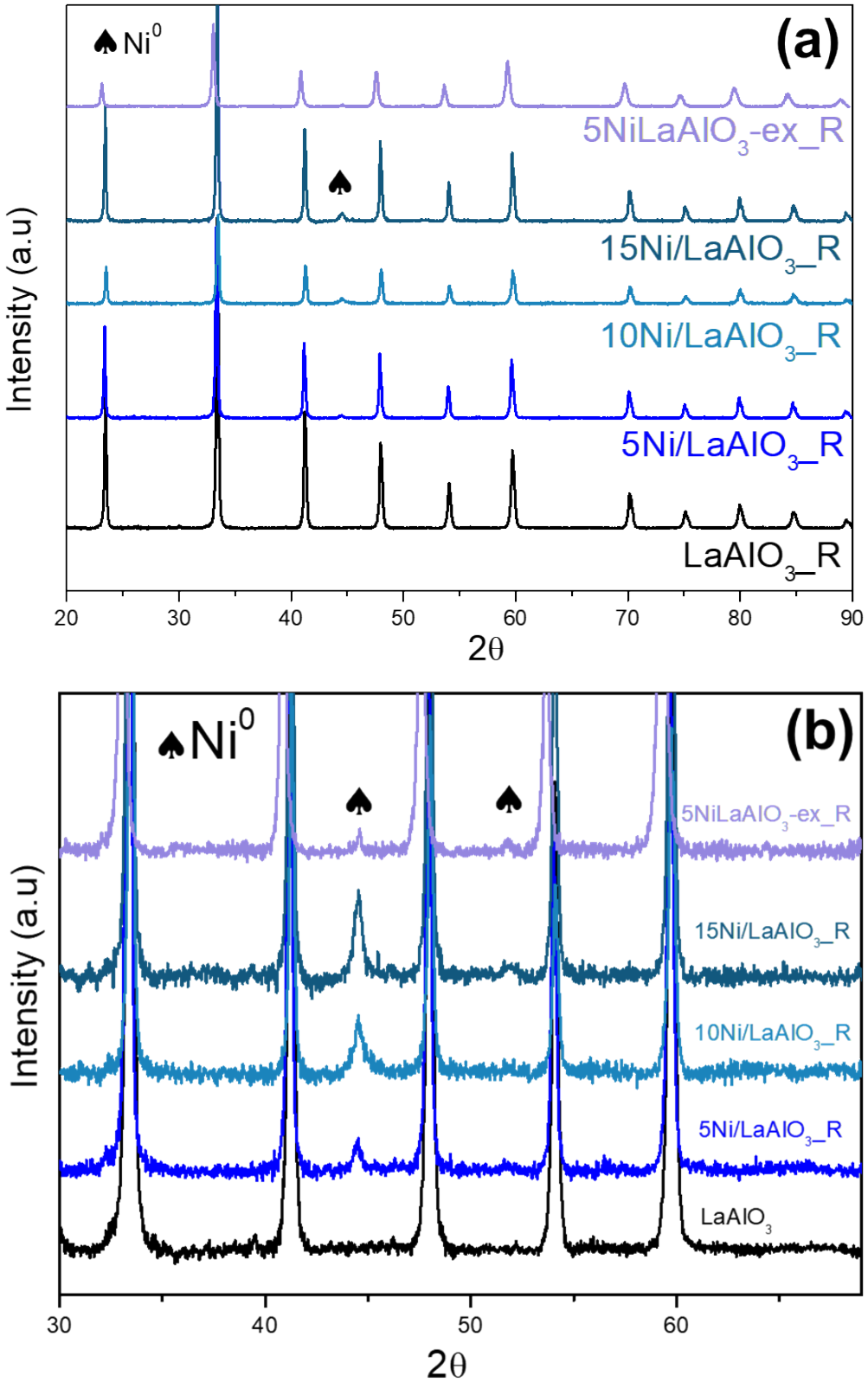

Figure S8. (a) XRD diffractograms of the reduced $LaAlO_3$-based catalysts. (b) Magnification of the region between 2θ = 30° and 70° to highlight the presence of diffraction peaks related to the presence of the Ni^0 phase.

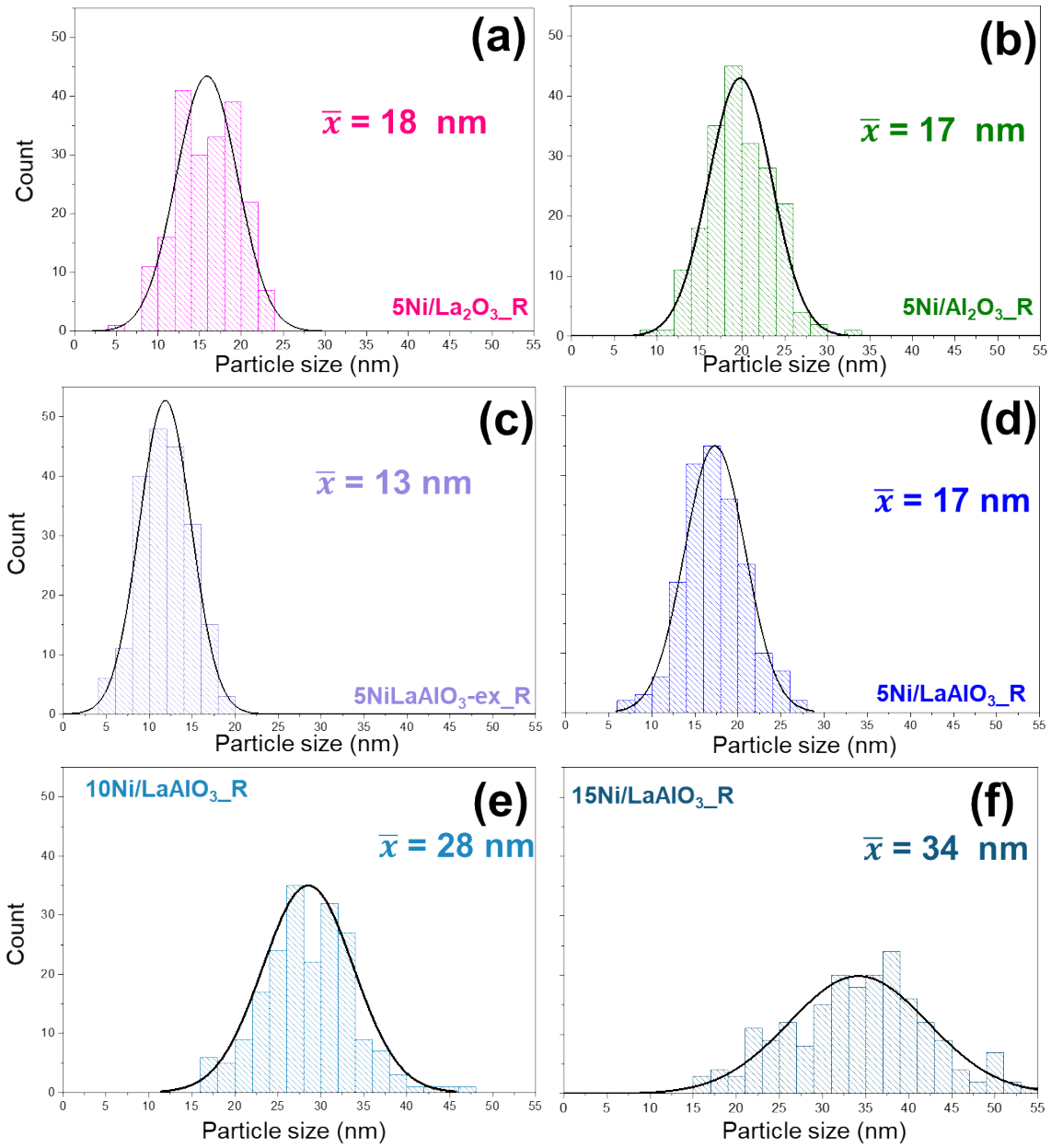

Figure S9. Size distribution for Ni^0 particles obtained, normal fit and average size for (a) $5Ni/La_2O_3\_R$; (b) $5Ni/Al_2O_3\_R$, (c) $5NiLaAlO_3$-ex_R, (d) $5Ni/LaAlO_3\_R$; (e) $10Ni/LaAlO_3\_R$, and (f) $15Ni/LaAlO_3\_R$. 200 particles were measured for each one using the TEM images treated with the ImageJ software.

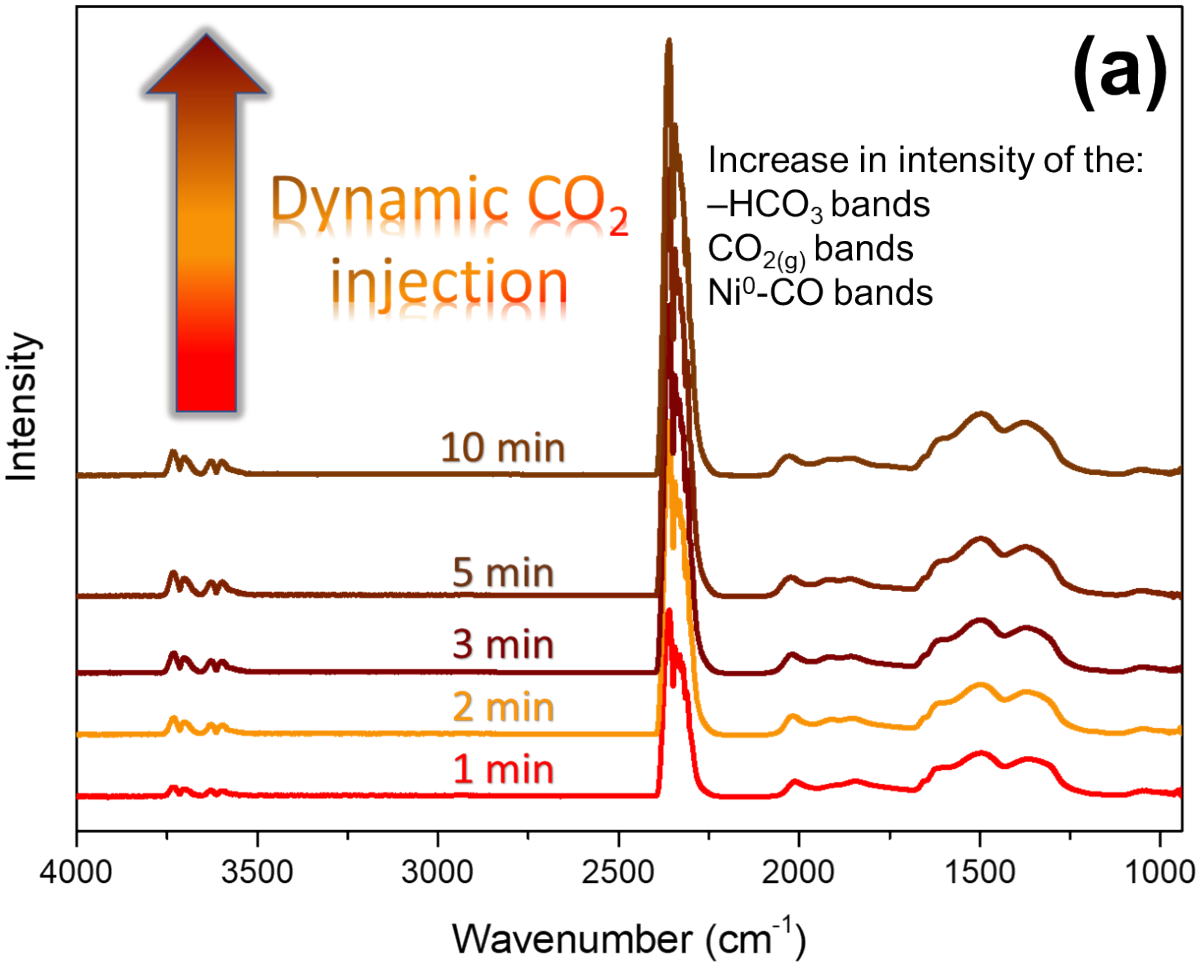
(a)
Dynamic CO_2 injection
Increase in intensity of the:
–HCO_3 bands
$CO_{2(g)}$ bands
Ni^0-CO bands
10 min
5 min
3 min
2 min
1 min
Intensity
4000
3500
3000
2500
2000
1500
1000
Wavenumber (cm^{-1})

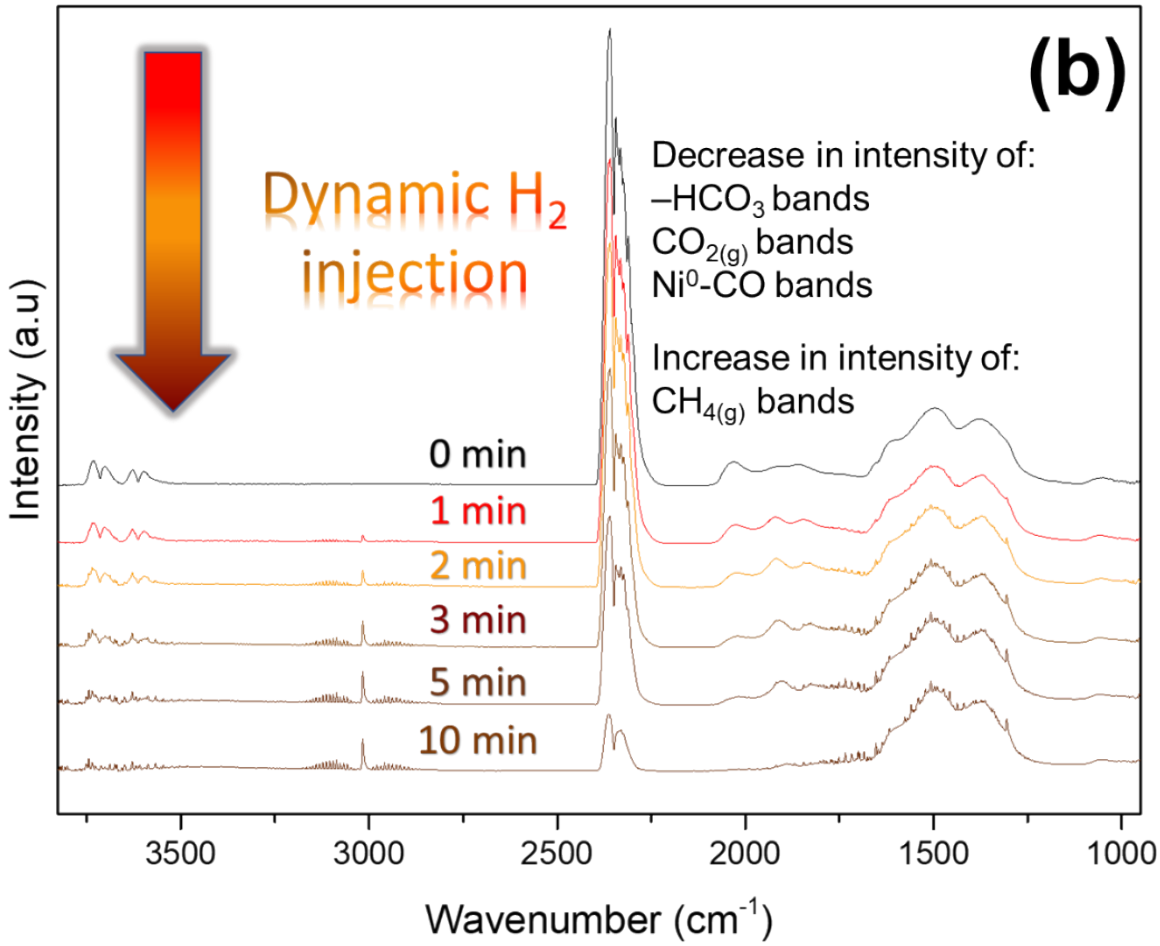

Figure S10. Time-resolved in-situ FT-IR transmission measurements for the 15Ni/$LaAlO_3$ catalyst during (a) CO_2 exposition and (b) subsequent H_2 exposition. Full range between 900 and 3800 cm^{-1}.

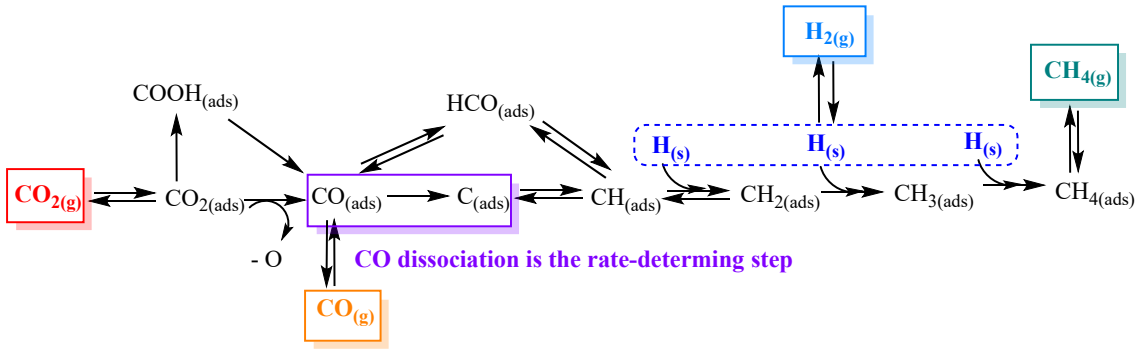

Figure S11. Simplified representation of the mechanistic pathways that might take for the CO_2 methanation, which can follow either the associative or the dissociative pathway.

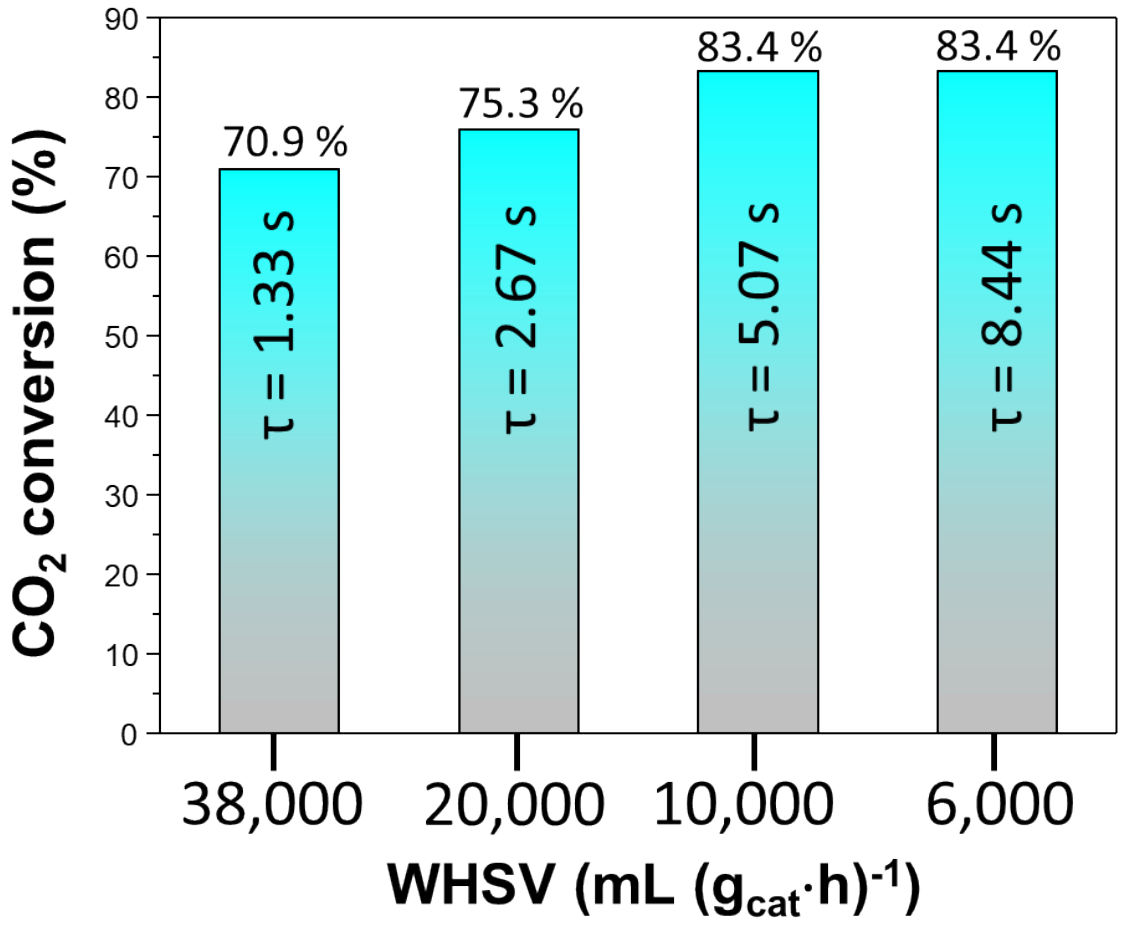

Figure S12. Dependence of CO_2 conversion as a function of the weight hourly speed velocity (WHSV). The corresponding time of contact (τ) of the reactants with the active phase is indicated. Reaction conditions: 320 °C, 1 atm, molar $H_2/CO_2 = 4$.

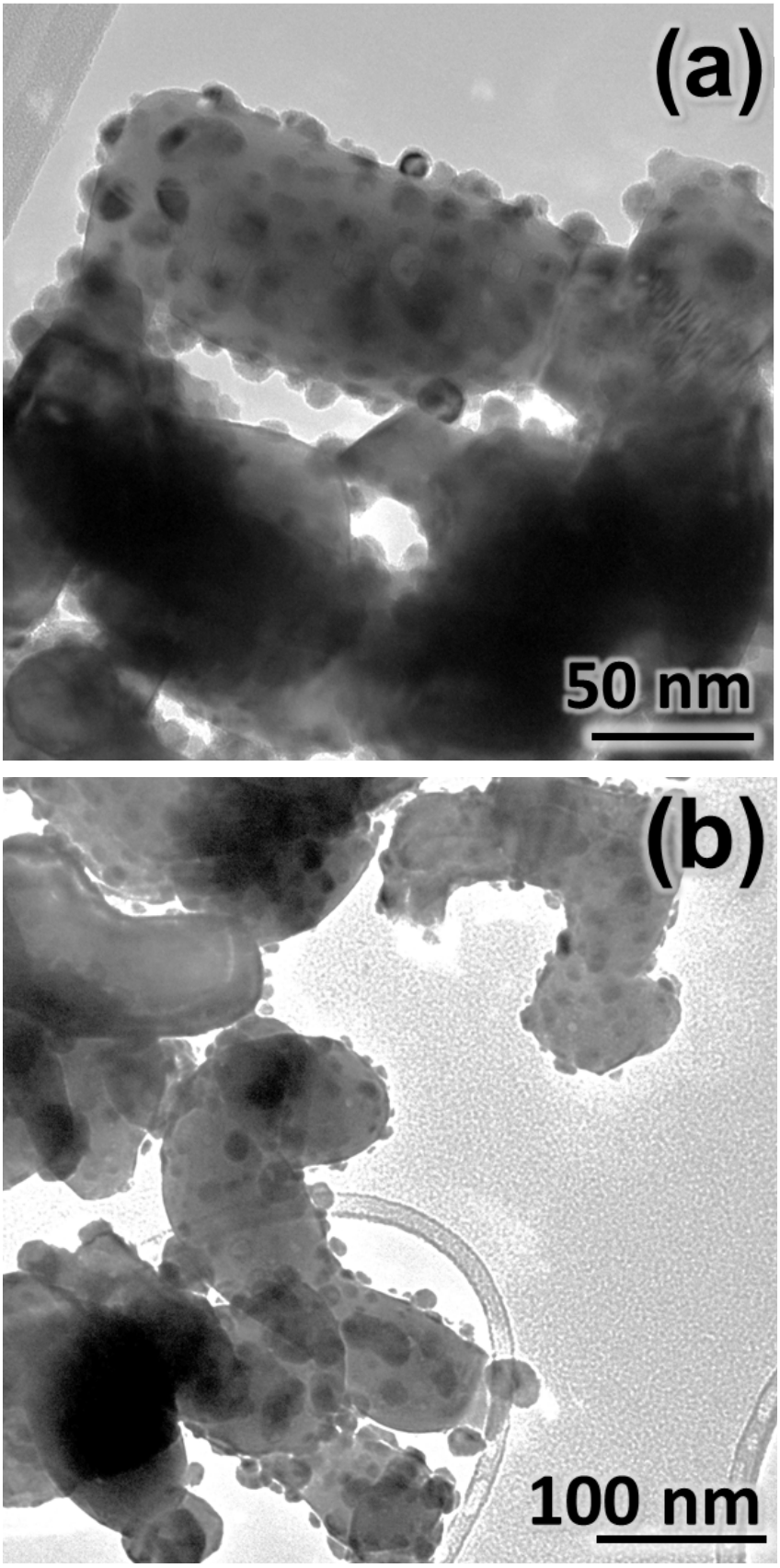

Figure S13. TEM images of the 15Ni/$LaAlO_3$<ST>, i.e., after the 12-hour stability tests in which the catalyst was employed for CO_2 methanation with a sweetened biogas sample.

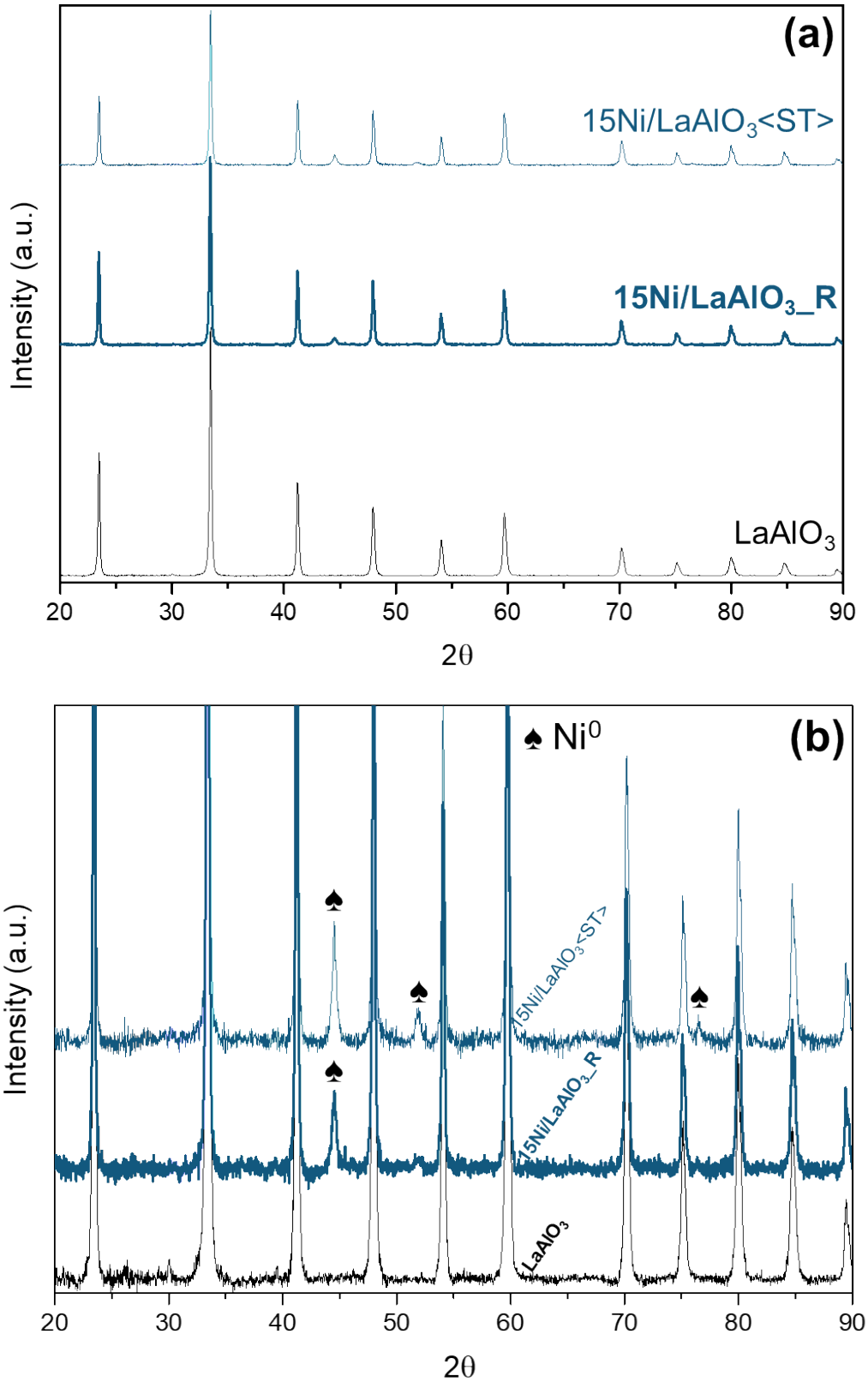

Figure S14. (a) XRD diffractogram of the 15Ni/$LaAlO_3$ catalyst after the stability test in comparison with the reduced catalyst and the bare support. (b) Zoom-in to highlight the presence of the Ni^0 phase peaks.

Table S1. Elemental weight percentage for lanthanum aluminate samples, as determined by ICP-OES , and La/Al molar ratio.

	La(%)	Al (%)	Ni (%)	La/Al molar ratio
La_2O_3	84.0	-	-	-
5Ni/La2O3	78.5	-	5.4	-
Al_2O_3	-	50.8	-	-
$5Ni/Al_2O_3$	-	47.5	5.6	-
$LaAlO_3$	64.7	12.7	n/a	0.987
$5Ni/LaAlO_3$	59.4	11.7	5.4	0.983
$10Ni/LaAlO_3$	57.1	11.0	10.8	1.007
$15Ni/LaAlO_3$	53.5	10.5	15.5	0.988
$5NiLaAlO_3$-ex	63.9	12.2	4.9	1.018

Table S2. CO_2-TPD deconvolution for the concentration of weak (50 – 150 °C), moderate (150-400 °C) and strong (400-900 °C) basic sites and total basicity for the different supports and catalysts.

Sample	Deconvolution (mmol CO_2 g^{-1})			Total basicity (mmol CO_2 g^{-1})
	Weak	Moderate (B_{CO2})	Strong	
Al_2O_3	0.08	1.31	0.24	**1.63**
La_2O_3	0.11	0.45	1.69	**2.25**
$LaAlO_3$	0	2.32	0.95	**3.27**
5Ni/Al_2O_3_R	0.04	0.91	1.35	**2.30**
5Ni/La_2O_3_R	0.05	0.62	1.40	**2.07**
5Ni$LaAlO_3$-ex_R	0	2.64	1.12	**3.76**
5Ni/$LaAlO_3$_R	0	3.03	1.25	**4.28**
10Ni/$LaAlO_3$_R	0	3.30	1.29	**4.59**
15Ni/$LaAlO_3$_R	0	3.36	1.26	**4.62**

Table S3. Vibration modes for different species in the 15Ni/$LaAlO_3$ catalyst and corresponding wavenumber.

Vibration mode	Wavenumber (cm^{-1})	Reference
linear Ni^0-CO	2026	Cárdenas-Arenas et al.[1]
bridge Ni^0-CO	1918	Cárdenas-Arenas et al.[1]
multi-bonded Ni^0-CO	1859	Cárdenas-Arenas et al.[1]
$CH_{4(g)}$	3016/1302	Cerdá Moreno et al.[2]
ν(C=O) monodentate carbonate	1653/1609	Cerdá Moreno et al.[2]
ν(C=O) bidentate carbonate	1495	Lorber et al. [3]
ν(C=O) formate	1378	Li et al.[4]

References

1. Cárdenas-Arenas, A.; Quindimil, A.; Davó-Quiñonero, A.; Bailón-García, E.; Lozano-Castelló, D.; De-La-Torre, U.; Pereda-Ayo, B.; González-Marcos, J. A.; González-Velasco, J. R.; Bueno-López, A., Isotopic and in situ DRIFTS study of the CO2 methanation mechanism using Ni/CeO2 and Ni/Al2O3 catalysts. *Applied Catalysis B: Environmental* **2020,** *265*, 118538.

2. Cerdá-Moreno, C.; Chica, A.; Keller, S.; Rautenberg, C.; Bentrup, U., Ni-sepiolite and Ni-todorokite as efficient CO2 methanation catalysts: Mechanistic insight by operando DRIFTS. *Applied Catalysis B: Environmental* **2020,** *264* (December 2019), 118546-118546.

3. Lorber, K.; Zavašnik, J.; Arčon, I.; Huš, M.; Teržan, J.; Likozar, B.; Djinović, P., CO2 Activation over Nanoshaped CeO2 Decorated with Nickel for Low-Temperature Methane Dry Reforming. *ACS Applied Materials & Interfaces* **2022,** *14* (28), 31862-31878.

4. Li, T.; Dong, M.; Xu, J.; Zhang, T.; Sun, Y.; Li, N.; Wu, Z.; Li, J.; Gao, E.; Zhu, J.; Yao, S.; Huang, Y., Exploring the Promotion of γ-Al2O3 on Pd/CeO2-Catalyzed Low-Concentration Methane Oxidation Using Operando DRIFTS-MS. *ChemCatChem* **2023,** *15* (7), e202300194.